



# Spherical collapse model in varying $G$ cosmologies

M. Taji<sup>1</sup> · M. Malekjani<sup>1</sup>

Received: 6 March 2019 / Accepted: 22 July 2019 / Published online: 26 July 2019  
© Springer Nature B.V. 2019

**Abstract** By using the spherical collapse model, we investigate the growth of perturbations in time varying  $G$  cosmologies. We study the transition redshift from early decelerated expansion to current accelerated phase in varying  $G$  theories. Applying the Chevallier-Polarski-Linder parameterization for dark energy, we study the effect of dark energy on the evolution of density perturbations in varying  $G$  cosmologies. The main quantities in spherical collapse model, the linear overdensity parameter  $\delta_c$  and the virial overdensity  $\Delta_{vir}$  are calculated. We compute the number of virialized dark matter haloes in the context of varying  $G$  cosmologies using the Sheth-Tormen mass function. Finally, we improve the spherical collapse model in varying  $G$  cosmologies by calculating the effects of shear and rotation on  $\delta_c$  and  $\Delta_{vir}$  and the modification of mass function on the number count of dark matter haloes.

**Keywords** Cosmology · Dark energy · Large scale structure in the universe

## 1 Introduction

In 1998, two independent groups (Riess et al. 1998; Perlmutter et al. 1999) measured the apparent magnitudes of Type I supernovae (SNeIa), which are known as the standard candles since their absolute magnitudes are the same. Their measurements reveal that the present phase

of the expansion of universe is the accelerated expansion (Jaffe et al. 2001; Riess et al. 2004; Tegmark et al. 2004; Percival et al. 2004; Kowalski et al. 2008; Jarosik et al. 2011; Komatsu et al. 2011). In fact, the luminosity distance calculated in a universe dominated by cold dark matter (CDM) is lower than the observed value at high redshifts. Not only the observations of high-redshift SNeIa, but also cosmic microwave background observations (CMB) (Ho et al. 2008; Komatsu et al. 2009; Jarosik et al. 2011) and baryon acoustic oscillations (BAO) (Eisenstein et al. 2005; Percival et al. 2010) indicate that the current expansion of universe is accelerated. In the context of General Relativity (GR), an exotic fluid with sufficiently negative pressure, the so-called dark energy (DE), is the source of this acceleration. Moreover, the results of the Planck experiments (Ade et al. 2014) indicate that DE occupies about two-thirds of the total energy density in the current universe. In the past two decades, many theoretical and phenomenological DE models were proposed to describe the accelerated phase of expanding universe. The earliest and simplest model is the Einstein's cosmological constant with constant equation of state (EoS)  $\omega_\Lambda = -1$  (Padmanabhan 2003). This model has two famous difficulties namely cosmic coincidence and fine-tuning problems (Weinberg 1989; Sahni and Starobinsky 2000; Carroll 2001; Peebles and Ratra 2003; Copeland et al. 2006). In order to alleviate these problems, some alternative DE models with time varying EoS parameter have been proposed (Kamenshchik et al. 2001; Armendariz-Picon et al. 2001; Caldwell 2002; Sen 2002; Thomas 2002; Linder 2003; Nojiri and Odintsov 2003; Arkani-Hamed et al. 2004; Piazza and Tsujikawa 2004; Cai 2007). DE has two important effects during the evolution of universe with cosmic time. Firstly, DE accelerates the expansion of the universe and secondly it changes the growth rate of cosmic structures. In fact, the observations indicate that the universe

✉ M. Malekjani  
malekjani@basu.ac.ir  
M. Taji  
m.taji@sci.basu.ac.ir

<sup>1</sup> Department of Physics, Bu-Ali Sina University, Hamedan 65178, Iran

is not homogeneous and isotropic on small scales. The inhomogeneous universe originates from primordial quantum density fluctuations at inflationary phase era (Starobinsky 1980; Guth 1981; Linde 1990). In the scenario of structure formation we follow the evolution of small initial density fluctuations during different phase of the evolution of universe until present time. In particular, we study how the cosmic structures like galaxies and cluster of galaxies can form from the initial density fluctuations due to the process of gravitational instability (Sheth and Tormen 1999; Barkana and Loeb 2001; Peebles and Ratra 2003; Ciardi and Ferrara 2005; Abramo et al. 2009; Bromm and Yoshida 2011; Appleby et al. 2013; Pace et al. 2014a). Generally, the growth of perturbations of a cosmic fluid on sub- Hubble scales depends on the Jeans length scale  $\lambda_J$ . On scales smaller than Jeans length scale ( $\lambda < \lambda_J$ ), perturbations can not grow and vanish, while on scales larger than Jeans length scale ( $\lambda_J < \lambda < H^{-1}$ ) perturbations can grow due to gravitational instability (Peebles 1993). The spherical collapse model (SCM) (Gunn and Gott 1972) is the semi-analytical method to study the growth of structure formation. In SCM, we consider a top-hat spherical overdense region with radius  $R$  inside the Hubble horizon. In this scale, the results of Pseudo Newtonian dynamics are well consistent with those of GR paradigm (Abramo et al. 2007, 2009). Due to self gravity, the spherical region expands slower than the background Hubble expansion. Hence the density inside the overdense region becomes higher than background and the expansion rate becomes slower. Finally, at a certain redshift, the so-called turnaround redshift  $z_{ta}$ , the spherical overdense region detaches from the Hubble flow and starts to collapse towards the center. At turnaround redshift  $z_{ta}$ , the region has a maximum radius  $R_{ta}$ . The collapsing sphere finally reaches the steady state at a virial radius  $R_{vir}$  in a certain redshift  $z_{vir}$ . In the framework of GR, the SCM has been investigated in several studies (Fillmore and Goldreich 1984; Bertschinger 1985; Hoffman and Shaham 1985; Ryden and Gunn 1987; Avila-Reese et al. 1988; Subramanian et al. 2000; Ascasibar et al. 2004; Williams et al. 2004; Mehrabi et al. 2017) Also, this model has been investigated for various DE and scalar field models (Mota and van de Bruck 2004; Maor and Lahav 2005; Basilakos and Voglis 2007; Abramo et al. 2007, 2009; Basilakos et al. 2009; Li et al. 2009; Pace et al. 2010; Wintergerst and Pettorino 2010; Basse et al. 2011; Pace et al. 2012, 2014a; Naderi et al. 2015; Malekjani et al. 2015b).

On the other hand, there are enough observational evidences which support the time variation of Newtons gravitational coupling  $G$  at Hubble scales  $H^{-1}$ . Observations of Binary Pulsar (Damour et al. 1988), Helio-seismological (Guenther et al. 1998), SNeIa (Gaztanaga et al. 2002), Astro-seismological (Benvenuto et al. 2004), Big Bang nucleosynthesis (Copi et al. 2004), Lunar Laser Ranging (Turyshev et al. 2004) confirm the variation of  $G$  with cosmic

time. For instance, SNeIa observations lead to  $-10^{-11} \leq \dot{G}/G < 0 \text{ yr}^{-1}$ , while Helio-seismological data give the bound of  $G$  as  $-1.6 \times 10^{-12} \text{ yr}^{-1} < \dot{G}/G < 0$ . From the theoretical point of view, the time varying  $G$  scenarios at cosmological scales can be proposed in the context of modified field equations. Notice that because of energy conservation law, the Einstein field equations do not permit any variations in the gravitational constant  $G$ , which couples to geometry and matter. However, in Brans-Dicke (Brans and Dicke 1961) and Kaluza-Klein (Kaluza 1921; Loren-Aguilar et al. 2003; Kolb et al. 1986; Maeda 1986; Freund 1982) theories, the variation of  $G$  has been predicted. The Brans-Dicke gravity makes the gravitational constant  $G$  as a dynamical field coupled to the matter component  $T^{\mu\nu}$  and is proportional to the inverse of gravitational coupling  $G$ . In Kaluza-Klein cosmology, we have  $(4 + 1)$  dimensional space-time in which the extra dimension is used to couple the gravity and electromagnetism. In these theories,  $G$  is replaced by a scalar function of time. In this paper, for the first time, we extend the SCM in varying  $G$  cosmological models. We consider the Chevallier-Polarski-Linder (CPL) parameterization (Chevallier and Polarski 2001; Linder 2003) for DE and investigate how DE affects the parameters of SCM in varying  $G$  cosmologies. We also calculate the number count of massive halo clusters in the context of varying  $G$  cosmology and compare the results with those of concordance  $\Lambda$ CDM universe. This paper is organized as follows. In Sect. 2, we study the varying  $G$  theories, then the modified Friedmann equations are obtained in varying  $G$  cosmologies. The SCM and the predicted number density of dark matter haloes in varying  $G$  cosmologies are presented in Sect. 3. Finally, our conclusions are presented in Sect. 4.

## 2 Varying $G$ theories

The total action in varying  $G$  theories (hereafter, VG theories) is described as: (Lu et al. 2014)

$$S = \frac{1}{16\pi} \int \sqrt{-g} \frac{R}{G(t)} d^4x + S_m, \quad (1)$$

where  $R = g^{\mu\nu} R_{\mu\nu}$  is the Ricci scalar,  $S_m$  is the action of matter and  $g$  is the determinant of the metric, i.e.,  $g = -|g|$ . The function  $G(t)$  is proportional to the inverse of a dynamical field  $\phi$ , which is coupled to the mass density of the universe.  $G(t)$  is usually written as  $G(t) = \phi^{-1} = G_0 a(t)^{-\beta}$ , where  $a(t)$  represents the scale factor,  $\beta$  is a constant parameter and  $G_0$  is the bare gravitational constant. Taking the variation of Eq. (1) with respect to gravitational field  $g_{\mu\nu}$ , field equations in VG theories are obtained as (Lu et al. 2014):

$$G_{\mu\nu} = R_{\mu\nu} - \frac{1}{2} R g_{\mu\nu}$$

$$= 8\pi GT_{\mu\nu} + G(\nabla_\mu \partial_\nu G^{-1} - g_{\mu\nu} \nabla_\rho \partial^\rho G^{-1}), \tag{2}$$

where  $R_{\mu\nu}$  denotes the Ricci tensor and  $T_{\mu\nu}$  is the energy-momentum tensor, which can be written for a perfect fluid as:

$$T^{\mu\nu} = P g^{\mu\nu} + (P + \rho)u^\mu u^\nu, \tag{3}$$

here  $u^\mu$  is the velocity four-vector satisfying  $u^\mu u_\mu = 1$ . In a flat FRW universe, the metric is written in the form of

$$ds^2 = dt^2 - a^2(t)[dr^2 + r^2(d\theta^2 + \sin^2\theta d\phi^2)]. \tag{4}$$

From the modified field equation (2) in the context of FRW metric, the modified Friedmann equations for VG universe dominated by pressureless matter and DE can be obtained as (Malekjani et al. 2015a):

$$H^2 = \frac{8\pi G(t)}{3(1 + \beta)}\rho \tag{5}$$

and

$$\frac{\ddot{a}}{a} = \frac{-4\pi G(t)}{3(1 + \beta/2)} \left[ \frac{(1 + \beta + \beta^2)}{(1 + \beta)}\rho + 3P \right], \tag{6}$$

where  $\rho = \rho_m + \rho_d$  and  $P = P_d$  are the total energy density and pressure of the fluid in the universe, respectively. Here subscript “ $m$ ” refers to all pressureless matter (baryons+dark matter) and subscript “ $d$ ” stands for DE component. Furthermore, The dot is the derivative with respect to the cosmic time. Note that in the case  $\beta = 0$ , the above modified Friedmann equations reduce to those of standard GR theory. In terms of dimensionless density parameters,

$$\Omega_m = \frac{\rho_m}{\rho_c}, \quad \Omega_d = \frac{\rho_d}{\rho_c}, \tag{7}$$

where  $\rho_c = 3H^2/8\pi G$  is the critical density, the first Friedmann equation (5) is written as

$$1 + \beta = \Omega_m + \Omega_d. \tag{8}$$

From Eq. (8), we see that in VG formalism, for a spatially flat FRW universe containing pressure-less matter and DE, the sum of dimensionless density parameters can be less (more) than one when  $\beta$  is negative (positive). Also the conservation law in an expanding VG universe reads (Lu et al. 2014; Malekjani et al. 2015a)

$$\dot{\rho} + 3H \left( \frac{6 + 2\beta + \beta^2}{6 + 3\beta} \rho + \frac{2 + 2\beta}{2 + \beta} P \right) = 0. \tag{9}$$

Clearly, by inserting  $\beta = 0$ , we get the standard continuity equation in standard gravity. The energy conservation

Eq. (9) can be separated in terms of pressureless matter and DE components as

$$\dot{\rho}_m + H \left( \frac{6 + 2\beta + \beta^2}{2 + \beta} \right) \rho_m = 0, \tag{10}$$

$$\dot{\rho}_d + 3H\rho_d \left( \frac{6 + 2\beta + \beta^2}{6 + 3\beta} + \frac{2 + 2\beta}{2 + \beta} \omega_d \right) = 0, \tag{11}$$

where  $\omega_d = P_d/\rho_d$  is the EoS parameter of DE. Now, we can integrate Eqs. (10) and (11) to find the energy densities for matter and DE as follows:

$$\rho_m = \rho_{m0} a^{-\frac{6+2\beta+\beta^2}{2+\beta}}, \tag{12}$$

$$\rho_d = \rho_{d0} a^{-\frac{6+2\beta+\beta^2}{2+\beta}} e^{-\frac{6+6\beta}{2+\beta} \left( \int_1^a \omega_d \frac{da}{a} \right)}. \tag{13}$$

Furthermore by combining Eqs. (12), (13) and (6), the dimensionless Hubble parameter  $E = H/H_0$  in VG theory is written as

$$E^2 = \frac{H^2}{H_0^2} = \frac{a^{-\frac{6+2\beta+\beta^2}{2+\beta}}}{1 + \beta} \left[ \Omega_{d0} e^{-\frac{6+6\beta}{2+\beta} \left( \int_1^a \omega_d \frac{da}{a} \right)} + \Omega_{m0} \right], \tag{14}$$

where  $\Omega_{m0} = (8\pi G/3H_0^2)\rho_{m0}$  and  $\Omega_{d0} = (8\pi G/3H_0^2)\rho_{d0}$ . Also, using Eqs. (5) and (9), we can obtain the deceleration parameter,  $q = -1 - \frac{\dot{H}}{H^2}$ , in VG formalism as

$$q = \frac{1}{2 + \beta} (1 + \beta + \beta^2 + 3\Omega_d \omega_d). \tag{15}$$

The positive sign of deceleration parameter ( $q > 0$ ) represents the decelerated expansion and negative sign ( $q < 0$ ) indicates the accelerated phase of expansion in the universe. Putting  $\beta = 0$ , the deceleration parameter is reduced to its ordinary form in the standard FRW cosmology with constant  $G$  as follows:

$$q = \frac{1}{2} (1 + 3\Omega_d \omega_d). \tag{16}$$

Combining Eqs. (7) and (13), we get

$$\Omega_d = \frac{\Omega_{d0}}{E^2} a^{-\frac{6+2\beta+\beta^2}{2+\beta}} e^{-\frac{6+6\beta}{2+\beta} \left( \int_1^a \omega_d \frac{da}{a} \right)}. \tag{17}$$

Now, we can rewrite Eq. (15) as

$$q = \frac{1}{2 + \beta} \times \left[ 1 + \beta + \beta^2 + 3\omega_d \frac{\Omega_{d0}}{E^2} a^{-\frac{6+2\beta+\beta^2}{2+\beta}} e^{-\frac{6+6\beta}{2+\beta} \left( \int_1^a \omega_d \frac{da}{a} \right)} \right]. \tag{18}$$

In the rest of the paper, we adopt the EoS parameter of DE as the Chevallier-Polarski-Linder (CPL) parameteriza-

**Table 1** Different DE models by considering the CPL parameterization in VG theory

Model	$\omega_0$	$\omega_1$	$\beta$
Model I	-1	1/3	-0.01
Model II	-1	1/3	+0.01
Model III	-2/3	0	-0.01
Model IV	-2/3	0	+0.01
Model V	-4/3	1/3	-0.01
Model VI	-4/3	1/3	+0.01

tion (Chevallier and Polarski 2001; Linder 2003)

$$\omega_d = \omega_0 + \omega_1(1 - a) = \omega_0 + \omega_1 \frac{z}{1 + z}, \tag{19}$$

where  $a = 1/(1 + z)$ . It is easy to show that this parameterization can be interpreted as a Taylor series with respect to  $(1-a)$ . This means that the CPL parameterization can be expanded to more general case by assuming the second order approximation, i.e.,  $\omega(a) = \omega_0 + \omega_1(1 - a) + \omega_2(1 - a)^2$  (Seljak et al. 2005). In this work, we consider three different types of DE models via CPL parameterization presented in Table 1. For each case, we consider the parameter  $\beta$  as  $+0.01$  and  $-0.01$ . These values are chosen based on observational constraints (Lu et al. 2014; Malekjani et al. 2015a; Alavirad and Malekjani 2014).

In Fig. 1, we show the evolution of  $\omega_d$ ,  $\Omega_d$  and deceleration parameter  $q$  as a function of redshift  $z$  for different DE models presented in Table 1. In the upper panel, we see that for DE models (I & II) the EoS parameter varies in the quintessence regime ( $-1 < \omega_d < -1/3$ ). While in DE models (V & VI), the EoS parameter evolves in phantom phase ( $\omega_d < -1$ ). In DE models (III & IV), the EoS parameter is a constant value in quintessence regime. By considering these DE models, we can calculate the effect of both quintessence and phantom like DE models on the evolution of expanding universe. In the middle panel the evolution of density of DE for each model is depicted. The line style and colors are referred in Legends. We see that in all models the fractional energy density of DE tends to zero at high redshifts. This result is expected since at enough high redshift the DE effect on the evolution of Universe is negligible. Also, concerning the phase of cosmic expansion we show the evolution of deceleration parameter  $q$  in bottom panel. We find that in all VG models, the sign of parameter  $q$  changes from positive to negative values at  $z \simeq 0.6$ . This result is in good agreement with observational predictions based on the cosmic chronometers  $H(z)$  data (Farooq et al. 2017; Capozziello et al. 2014, 2015).

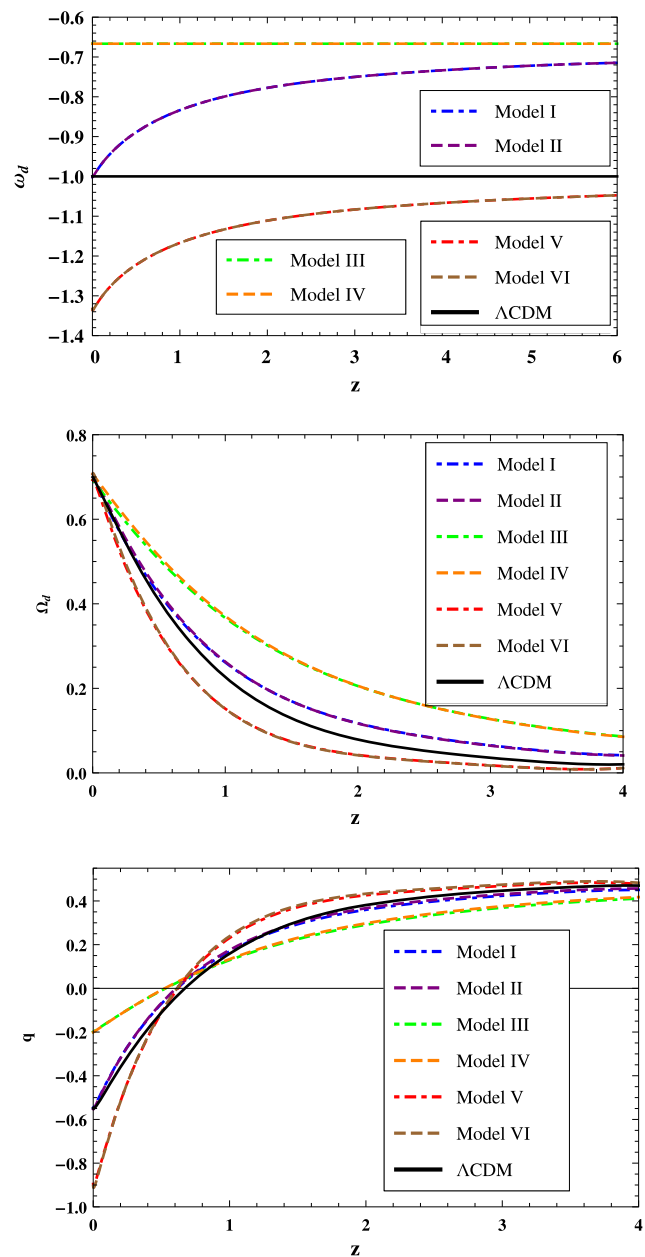


**Fig. 1** The redshift evolution of EoS parameter  $\omega_d(z)$  (top panel),  $\Omega_d(z)$  (middle panel) and deceleration parameter  $q$  (bottom panel) in VG cosmologies

### 3 Spherical collapse model

In this section we first present the basic equations of the SCM in VG theory and then calculate the SCM parameters in this theory. After that, the number of massive dark matter haloes are counted in VG gravity. Finally we improve our study by adding the shear and rotation as well as adopting a different mass function to calculate the SCM parameters and dark matter halo numbers in VG theory.

### 3.1 Basic equations

The matter density contrast  $\delta_m(t)$  for spherical region is defined as

$$\delta_m(t) = \frac{\rho_{mc}(t) - \rho_m(t)}{\rho_m(t)}. \tag{20}$$

Here  $\rho_{mc}$  is the matter density inside the spherical region and  $\rho_m$  denotes the matter density for the background. Moreover, since the distribution of DE is uniform, this means that the density of DE within the sphere is equal to the density of DE in background, i.e.  $\rho_d = \rho_{dc}$ . Thus, DE perturbations is vanishing everywhere under the influence of pressure. If  $\delta$  is positive, then the overdense regions will finally collapse (Bernardeau 1994; Padmanabhan 1996; Wang and Steinhardt 1998; Ohta et al. 2003, 2004; Linder 2005; Nesseris and Perivolaropoulos 2008). However, a negative density contrast corresponds to the under-dense regions, called voids, which expand faster than Hubble flow. Note that, the second Friedmann Eq. (6) can be applied for the dynamics inside the overdense region, replacing the scale factor  $a$  by radius  $r$  (Abramo et al. 2007). Thus, we have

$$\frac{\ddot{r}}{r} = \frac{-4\pi G(t)}{3(1 + \beta/2)} \left[ \frac{(1 + \beta + \beta^2)}{(1 + \beta)} \rho_c + 3P_c \right], \tag{21}$$

where  $\rho_c$  and  $P_c$  are, respectively, the total energy density and pressure of the fluid within the sphere. Also, the continuity Eq. (10) for the evolution of matter inside the perturbed region is written as

$$\dot{\rho}_{mc} + h \left( \frac{6 + 2\beta + \beta^2}{2 + \beta} \right) \rho_{mc} = 0, \tag{22}$$

where  $h$  is the local expansion rate inside the spherical region, which obeys the relation  $h = \dot{r}/r$ . Now, taking the time derivative of Eq. (20) and using the continuity Eqs. (10) and (22), we find

$$\dot{\delta}_m + \left( \frac{6 + 2\beta + \beta^2}{2 + \beta} \right) (1 + \delta_m)(h - H) = 0, \tag{23}$$

where over dot denote derivative with respect to cosmic time. The second derivative then gives

$$\delta_m \ddot{\delta}_m - \frac{\dot{\delta}_m^2}{1 + \delta_m} - (1 + \delta_m) \left( \frac{6 + 2\beta + \beta^2}{2 + \beta} \right) (\dot{H} - \dot{h}) = 0. \tag{24}$$

To complete the derivations, we first need to compute  $\dot{H} - \dot{h}$ . Therefore, using Eqs. (6) and (21) we can obtain

$$\begin{aligned} \dot{H} - \dot{h} &= \left( \frac{\ddot{a}}{a} - H^2 \right) - \left( \frac{\ddot{r}}{r} - h^2 \right) \\ &= h^2 - H^2 + \frac{1 + \beta + \beta^2}{(1 + \beta)(2 + \beta)} \delta_m \Omega_m H^2. \end{aligned} \tag{25}$$

In the above equation, we use the relation  $\rho_{mc} - \rho_m = -\delta_m \rho_m$  and we ignore the DE perturbation inside the perturbed region. Combining Eqs. (24) and (25), we find the equation which describes the evolution of density contrast in VG cosmology as follows:

$$\begin{aligned} \delta_m \ddot{\delta}_m - \left( \frac{8 + 3\beta + \beta^2}{6 + 2\beta + \beta^2} \right) \frac{\dot{\delta}_m^2}{1 + \delta_m} + 2H \dot{\delta}_m \\ - \frac{(6 + 2\beta + \beta^2)(1 + \beta + \beta^2)}{(1 + \beta)(2 + \beta)^2} \Omega_m H^2 (1 + \delta_m) \delta_m = 0. \end{aligned} \tag{26}$$

Using the relations

$$\begin{aligned} \dot{\delta}_m(t) &= aH(a)\delta'_m(a), \\ \ddot{\delta}_m(t) &= a^2 H^2(a)\delta''_m(a) + aH^2(a)\delta'_m(a) \\ &\quad + a^2 H(a)H'(a)\delta'_m(a), \end{aligned}$$

where the prime here is derivative with respect to the scale factor  $a$ , we can rewrite Eq. (26) in the following form:

$$\begin{aligned} \delta_m \ddot{\delta}_m + \left( \frac{3}{a} + \frac{E'}{E} \right) \delta'_m - \left( \frac{8 + 3\beta + \beta^2}{6 + 2\beta + \beta^2} \right) \frac{\delta'^2_m}{1 + \delta_m} \\ - (1 + \delta_m) \delta_m \\ \times \left[ \frac{(6 + 2\beta + \beta^2)(1 + \beta + \beta^2)}{(1 + \beta)(2 + \beta)^2} \frac{\Omega_{m0}}{E^2} a^{-\left(\frac{10+4\beta+\beta^2}{2+\beta}\right)} \right] \\ = 0. \end{aligned} \tag{27}$$

Note that to obtain the above equation, we use  $\Omega_m = (\Omega_{m0}/E^2)a^{-\left(\frac{6+2\beta+\beta^2}{2+\beta}\right)}$ . Ignoring the non-linear terms in this equation, the linear equation for the growth of overdensities in VG theory is obtained as

$$\begin{aligned} \delta_m \ddot{\delta}_m + \left( \frac{3}{a} + \frac{E'}{E} \right) \delta'_m \\ - \left[ \frac{(6 + 2\beta + \beta^2)(1 + \beta + \beta^2)}{(1 + \beta)(2 + \beta)^2} \frac{\Omega_{m0}}{E^2} a^{-\left(\frac{10+4\beta+\beta^2}{2+\beta}\right)} \delta_m \right] \\ = 0. \end{aligned} \tag{28}$$

It is easy to see that by putting  $\beta = 0$ , Eq. (27) reduces to its standard form as follows (Abramo et al. 2007; Pace et al. 2010; Malekjani et al. 2017):

$$\begin{aligned} \delta_m \ddot{\delta}_m + \left( \frac{3}{a} + \frac{E'}{E} \right) \delta'_m - \frac{4\delta'^2_m}{3(1 + \delta_m)} \\ - \frac{3\Omega_{m0}}{2E^2 a^5} (1 + \delta_m) \delta_m = 0. \end{aligned} \tag{29}$$

### 3.2 SCM parameters in VG theory

Now we determine the two main quantities of SCM, the linear overdensity  $\delta_c$  and the virial overdensity parameter

$\Delta_{vir}$ , in the context of VG cosmologies. The importance of quantity  $\delta_c$  is that it is used, together with the linear growth factor  $D(z)$ , to calculate the number density of virialized dark matter haloes. On the other hand, the virial overdensity  $\Delta_{vir}$  is used to determine the size of virialized haloes (Lahav et al. 1991; Wang and Steinhardt 1998; Mota and van de Bruck 2004; Horellou and Berge 2005; Wang and Tegmark 2005; Abramo et al. 2007; Basilakos and Voglis 2007; Pace et al. 2010, 2012; Batista and Pace 2013; Pace et al. 2014a; Malekjani et al. 2015b; Pace et al. 2014b; Naderi et al. 2015). In order to calculate these quantities, we follow the approach presented in (Pace et al. 2010). To evaluate  $\delta_c$ , we first need to solve the nonlinear Eq. (27) numerically, starting from an initial condition at initial scale factor  $a_i$ . Since at collapse scale factor  $a_c$ , the overdense sphere falls to its center, the overdensity  $\delta_m$  actually becomes infinite. Therefore, we should find an initial matter overdensity  $\delta_{mi}$  at the initial scale factor  $a_i$  to solve nonlinear Eq. (27) such that the final value of  $\delta_m$  at  $a_c$  becomes infinite. We fix the initial scale factor at  $a_i = 10^{-4}$  indicating the start of matter dominated universe. Beside  $\delta_{mi}$ , we set  $\delta'_{mi} = \delta_{mi}/a_i$  (Malekjani et al. 2015b, 2017; Rezaei and Malekjani 2017). Numerically, we assume the infinite value of  $\delta_m$  at  $a_c$  is achieved when  $\delta_m > 10^7$ . Once  $\delta_{mi}$  is found, we use it together with  $\delta'_{mi}$  to solve the linear Eq. (28) from initial scale factor  $a_i$  up to final scale factor  $a_c$ . The value of  $\delta_m$  at collapse scale factor  $a_c$  obtained from linear Eq. (28) is defined as linear overdensity  $\delta_c$  (Malekjani et al. 2015b; Nazari-Pooya et al. 2016) In the Einstein de-Sitter (EdS) universe, the linear overdensity  $\delta_c$  is equal to 1.686 independent of redshift  $z$ . In the case of  $\Lambda$ CDM cosmology, this value at present time is 1.675. Fig. 2 shows the evolution of linear overdensity  $\delta_c$  as a function of the collapse redshift  $z_c$  in VG theory for two different parameters  $\beta = -.01$  and  $\beta = .01$  where the EoS parameter of DE is considered by Eq. (19). The upper panel represents the quintessence regime, namely the effective EoS parameter obeys  $\omega_d > -1$ . The middle panel shows the solution for the VG model with constant EoS parameter  $\omega_d = -2/3$ . Finally, the lower panel refers to the phantom regime which has the EoS parameter  $\omega_d < -1$ . Here we fix the present values of DE density and matter density parameters as  $\Omega_{d0} \simeq .7$  and  $\Omega_{m0} \simeq .3$ , respectively. It can be seen that at low redshifts, when the universe is influenced by DE,  $\delta_c$  for all models is smaller than the value obtained at high redshifts. Eventually  $\delta_c$  tends to the EdS value at enough high redshifts when the universe is dominated by matter and the growth of structures is not affected by DE. Totally, the behavior of the evolution of linear overdensity  $\delta_c$  in VG theory is compatible with that if the DE cosmologies in GR theory (Devi and Sen 2011; Pace et al. 2010; Batista and Pace 2013).

Now we calculate the virial overdensity  $\Delta_{vir}$  in VG theory. In addition to determination the size of overdense region,  $\Delta_{vir}$  describes the ratio of the matter density in the

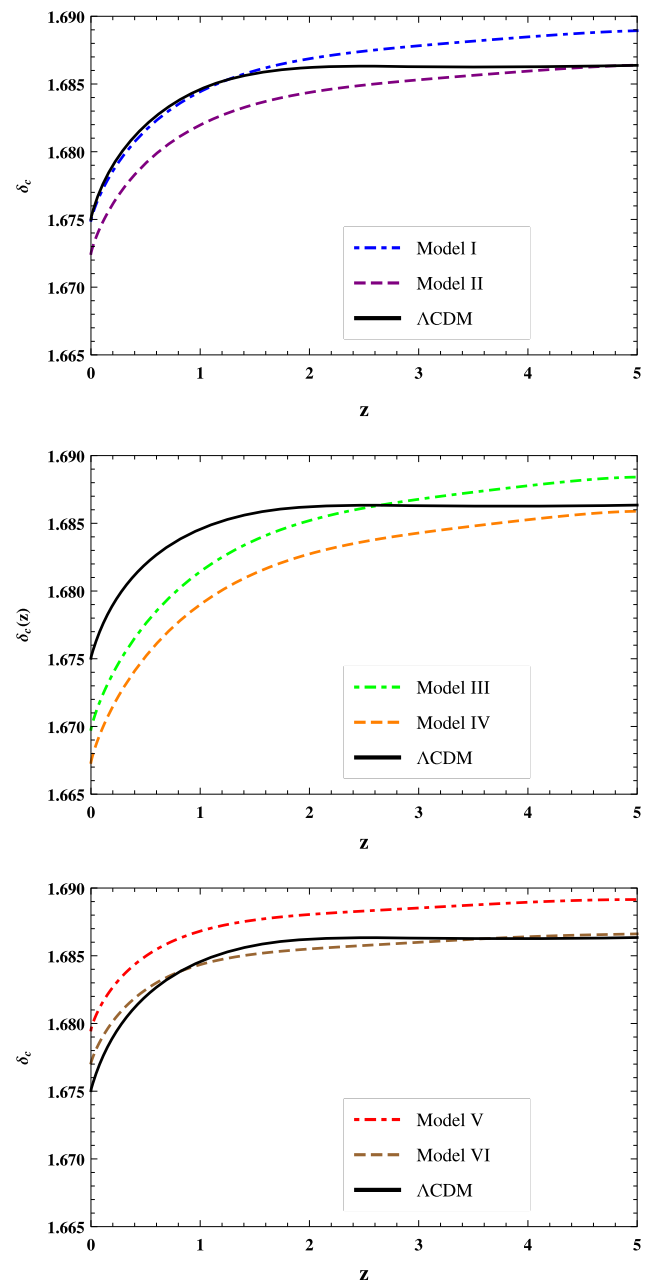


**Fig. 2** The evolution of the linear overdensity  $\delta_c(z)$  as a function of cosmic redshift  $z$  in VG cosmologies. Line style and colours are same as in Fig. 1

virialized structure to the background matter density at the same epoch and is defined as  $\Delta_{vir} = \xi(x/y)^3$ , where  $x$  is the scale factor normalised to the turn-around scale factor,  $y$  is the ratio between the radius of the sphere at  $z = z_{ta}$  and at virialization,  $y = R_{vir}/R_{ta}$ . The turn-around scale factor  $a_{ta}$  can be easily computed by finding the minimum of quantity  $\log(\frac{\delta_{nl}+1}{a^3})$  where  $\delta_{nl}$  is the non-linear overdensity. The value of density contrast at turnaround redshift can be obtained as  $\xi = \rho_{mc}(a_{ta})/\rho_m(a_{ta}) = \delta_{nl}(a_{ta}) + 1$  (Wang and Steinhardt 1998). Once  $\xi$  is obtained, we can calculate the

virial overdensity parameter using  $\Delta_{vir} = \xi(x/y)^3$ . In the limiting case of EdS universe, using the fact that the time of virialization is twice the turn-around time,  $t_{vir} = 2t_{ta}$ , it is easy to show that  $(a_c/a_{ta})_{EdS} = (1 + z_{ta})/(1 + z_c) = (t_c/t_{ta})^{2/3} = 2^{2/3} = 1.587$ , hence  $y = 1/2$ ,  $\xi = (3\pi/4)^2 \simeq 5.6$  and  $\Delta_{vir} \simeq 18\pi^2 \simeq 178$ . This result is independent of cosmic redshift which means that the collapse of structures takes place uniformly in the history of universe. However, this is not the case for DE cosmologies. In particular, DE can influence the virialization of structures at low redshifts. The effect of such a DE fluid is that the final radius of virialized halo will be larger or smaller than half of the turn-around radius and the sphere can reach to the equilibrium state with a larger or smaller radius that  $y = 1/2$ . Therefore in DE cosmologies, the SCM quantities vary by collapse redshift (Lahav et al. 1991; Wang and Steinhardt 1998; Mota and van de Bruck 2004; Horellou and Berge 2005; Wang and Tegmark 2005; Pace et al. 2014b; Malekjani et al. 2015b). In fact, in DE cosmologies, since  $\Delta_{vir}$  depends on the evolution of the DE component, it is a quantity depending on the redshift. In other words, according to whether DE takes part or not into the virialization process, the quantity  $y$  may be larger or smaller than  $1/2$  and the parameter  $\Delta_{vir}$  can be affected by including the DE sector (Pace et al. 2014b). This feature can be generalized when we consider DE in VG theory. In Fig. 3, we calculate the virial overdensity  $\Delta_{vir}$  in VG formalism for two different values of parameter  $\beta$ . As shown in the top panel, our results are closer to the reference  $\Lambda$ CDM model. In middle and bottom panels, the difference between  $\Lambda$ CDM model and VG models at the present time is bigger than top panel. In all models,  $\Delta_{vir}$  reaches the fiducial value  $\Delta_{vir} \simeq 178$  at high redshifts. Note that, at high redshifts, since the effect of DE fluid on the growth of structures is negligible,  $\Delta_{vir}$  increases to its EdS value for all models.

### 3.3 Haloes number counts

In this section, we compute the number counts of cluster-size dark matter haloes in the context of the VG cosmologies. The Press-Schechter formalism (Press and Schechter 1974) assumes that the abundance of virialized haloes can be expressed in terms of their mass. In this formalism, The comoving number densities of collapsed haloes with masses in the range of  $M$  and  $M + dM$  can be written as (Bond et al. 1991):

$$\frac{dn(M, z)}{dM} = \frac{\rho_{m0}}{M} \frac{d \ln \sigma^{-1}(M, z)}{dM} f(\sigma), \tag{30}$$

where  $\rho_{m0}$  is the matter density of the background at the present time,  $\sigma$  is the rms of the mass fluctuation in spheres containing the mass  $M$  and  $f(\sigma)$  is the mass function. The earliest and simplest mass function is the Press-Schechter

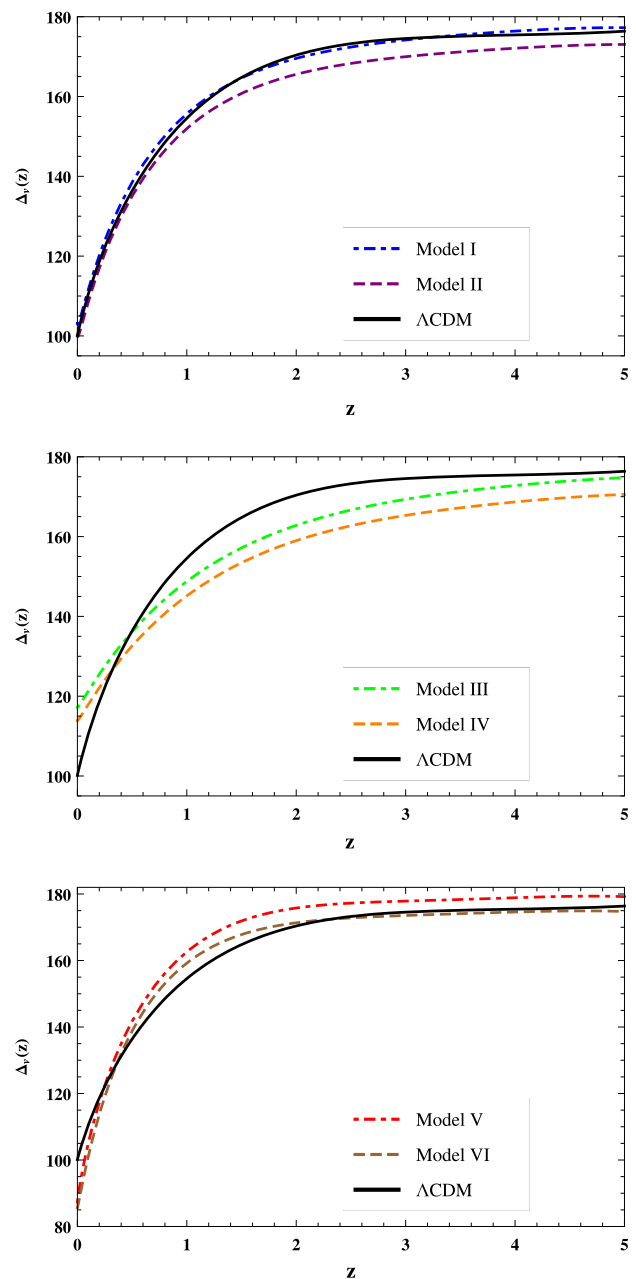


**Fig. 3** The evolution of the virial overdensity  $\Delta_{vir}$  with respect to the collapse redshift for the VG theory considering the CPL parameterization for DE. Line style and colours are same as in Fig. 1

(PS) mass function presented by (Press and Schechter 1974) as follows:

$$f(\sigma) = \sqrt{\frac{2}{\pi}} \frac{\delta_c(z)}{\sigma(M, z)} \exp\left[-\frac{\delta_c^2(z)}{2\sigma^2(M, z)}\right]. \tag{31}$$

The PS mass function gives a good general result, especially when the number density of intermediate size haloes is calculated. But this mass function fails to calculate the number density of high and low mass haloes. In fact it underpredicts high mass objects and overpredicts low mass objects at the

present epoch (Sheth and Tormen 1999; Jenkins et al. 2001; Sheth and Tormen 2002; Lima and Marassi 2004). So it is popular to use another fitting formula proposed by Sheth-Tormen (ST mass function) as (Sheth and Tormen 1999, 2002; Jenkins et al. 2001; Reed et al. 2007)

$$f_{ST}(\sigma) = A \sqrt{\frac{2a}{\pi}} \left[ 1 + \left( \frac{\sigma^2(M, z)}{a\delta_c^2(z)} \right)^p \right] \frac{\delta_c(z)}{\sigma(M, z)} \times \exp \left[ -\frac{a\delta_c^2(z)}{2\sigma^2(M, z)} \right]. \tag{32}$$

It is easy to see that ST mass function reduces to standard mass function by setting  $A = 1/2$ ,  $a = 1$  and  $p = 0$ . However, in ST mass function these numerical values read  $A = 0.3222$ ,  $a = 0.707$  and  $p = 0.3$ . Hence Eq. (30) can be written as

$$\frac{dn(M, z)}{dM} = \frac{\rho_{m0}}{M} \frac{dv}{dM} \left[ 0.2709 \sqrt{\frac{2}{\pi}} (1 + 1.1096v^{-0.6}) \right] \times \exp \left[ -\frac{0.707v^2}{2} \right], \tag{33}$$

where  $v(M, z) = \delta_c(z)/\sigma(M, z)$  and  $\delta_c(z)$  is the linear overdensity parameter. The quantity  $\sigma(M, z)$  is the variance of mass scale  $M$  at redshift  $z$  and can be calculated as (Abramo et al. 2007)

$$\sigma(M, z) = D(z)\sigma_M(z = 0), \tag{34}$$

where  $D(z) = \delta_m(z)/\delta_m(z = 0)$  is the linear growth factor computed from Eq. (28). Furthermore, we can calculate  $\sigma_M$  by using the following relation between  $\sigma_M$  and  $\sigma_8$  (Viana and Liddle 1996)

$$\sigma_M = \sigma_8 \left( \frac{M}{M_8} \right)^{-\gamma(M)/3}, \tag{35}$$

where  $\sigma_8$  is the rms of the mass fluctuation on the scale of size  $R_8 = 8h^{-1}$  Mpc at present time. Also  $M_8 = 6 \times 10^{14} \Omega_{m0} h^{-1} M_\odot$  is the mass inside  $R_8$  (Abramo et al. 2007). In order to calculate  $\sigma_8$  in VG theory we can use the relation  $\sigma_{8, VG} = [\delta_{c, VG}(z = 0)/\delta_{c, \Lambda CDM}(z = 0)]\sigma_{8, \Lambda CDM}$  where we use the Planck observational value for  $\sigma_{8, \Lambda CDM}$  as 0.815 (Ade et al. 2016). The exponent  $\gamma(M)$  in Eq. (35) is given by

$$\gamma(M) = (0.3\Gamma + 0.2) \left( 2.92 + \frac{1}{3} \log \frac{M}{M_8} \right), \tag{36}$$

where  $\Gamma = \Omega_{m0} h \exp(-\Omega_b - \Omega_b/\Omega_{m0})$ , is a shape parameter representing the profile of mass distribution inside the virialized haloes. To obtain the number density of virialized haloes with mass above a given value  $M_1$  at collapse redshift

$z$ , we integrate Eq. (33) from  $M_1$  to  $M_\infty$

$$n(> M_1, z) = \int_{M_1}^{M_\infty} \frac{dn}{dM} dM, \tag{37}$$

where we fix  $M_\infty$  to  $10^{18} M_\odot h^{-1}$  as such a gigantic structure could not be observed today. In this section, we compute the number density of collapsed haloes with mass above a typical value  $M_1$  from low mass tail ( $M_1 \equiv 10^{13} M_\odot h^{-1}$ ) to high mass tail ( $M_1 \equiv 10^{15} M_\odot h^{-1}$ ) of halo clusters by using the ST mass function. In terms of  $M_8$ , this range belongs to  $0.05 < M/M_8 < 5.55$ . In Figs. 4, 5 and 6, we display the abundance of number of collapsed haloes as a function of  $M/M_8$  computed in VG theory ( $n_{model}$ ) normalized to its value calculated in standard  $\Lambda$ CDM model ( $n_{\Lambda CDM}$ ). Various panels in Figs. 4, 5 and 6 from up to down are shown for different cosmic redshifts,  $z = 0$ ,  $z = 0.5$ ,  $z = 1$  and  $z = 2$ , respectively. Line style and colors are referred in the caption of figures. In each figure, we can observe the effect of DE as well as VG parameter  $\beta$  on the predicted number density of haloes based on the DE models presented in Table 1. Comparing different panels in each figure indicates the variation of these effects by varying redshift  $z$ . On the other hand comparing different figures, one can observe the effect of different DE models on the computed number density in VG cosmologies. Since we enforce all the models to share the same normalization of matter power spectrum  $\sigma_8$  at the present time, all VG models and  $\Lambda$ CDM cosmology have the same number of objects at  $z = 0$ . At  $z = 0.5$ , we see that all models including the  $\Lambda$ CDM one give roughly the same number of haloes at low mass tail ( $M = 10^{13} M_\odot/h$ ), while at high mass tail ( $M = 10^{15} M_\odot/h$ ) the differences between the VG models and concordance  $\Lambda$ CDM one are more pronounced. Quantitatively speaking, at  $z = 0.5$ , model I (model II) has roughly 6% (3%) more haloes than the  $\Lambda$ CDM model. This value is approximately 30% (28%) for model III (model IV) and  $-17\%$  ( $-19\%$ ) for model V (model VI). At higher redshifts,  $z = 1$  and  $z = 2$ , the differences between VG cosmological models and concordance  $\Lambda$ CDM universe appears also at low mass tail. We observe that models I, II, III and IV predict a higher number of virialized haloes compared to  $\Lambda$ CDM model. While models V and VI result a lower number of objects compare to  $\Lambda$ CDM universe. The above result is due to the behavior of DE and its effect on the abundance of virialized haloes. In fact for models I, II, III and IV, DE has the quintessence like EoS parameter (see Fig. 1), while in models V and VI, the EoS parameter of DE is phantom like. We can also observe the effect of VG parameter  $\beta$  on the predicted number of haloes. In all Figs. 4, 5 and 6, one can see that models I, III and V with negative VG parameter ( $\beta = -0.01$ ) has more virialized haloes than models II, IV and VI with positive VG parameter ( $\beta = +0.01$ ).



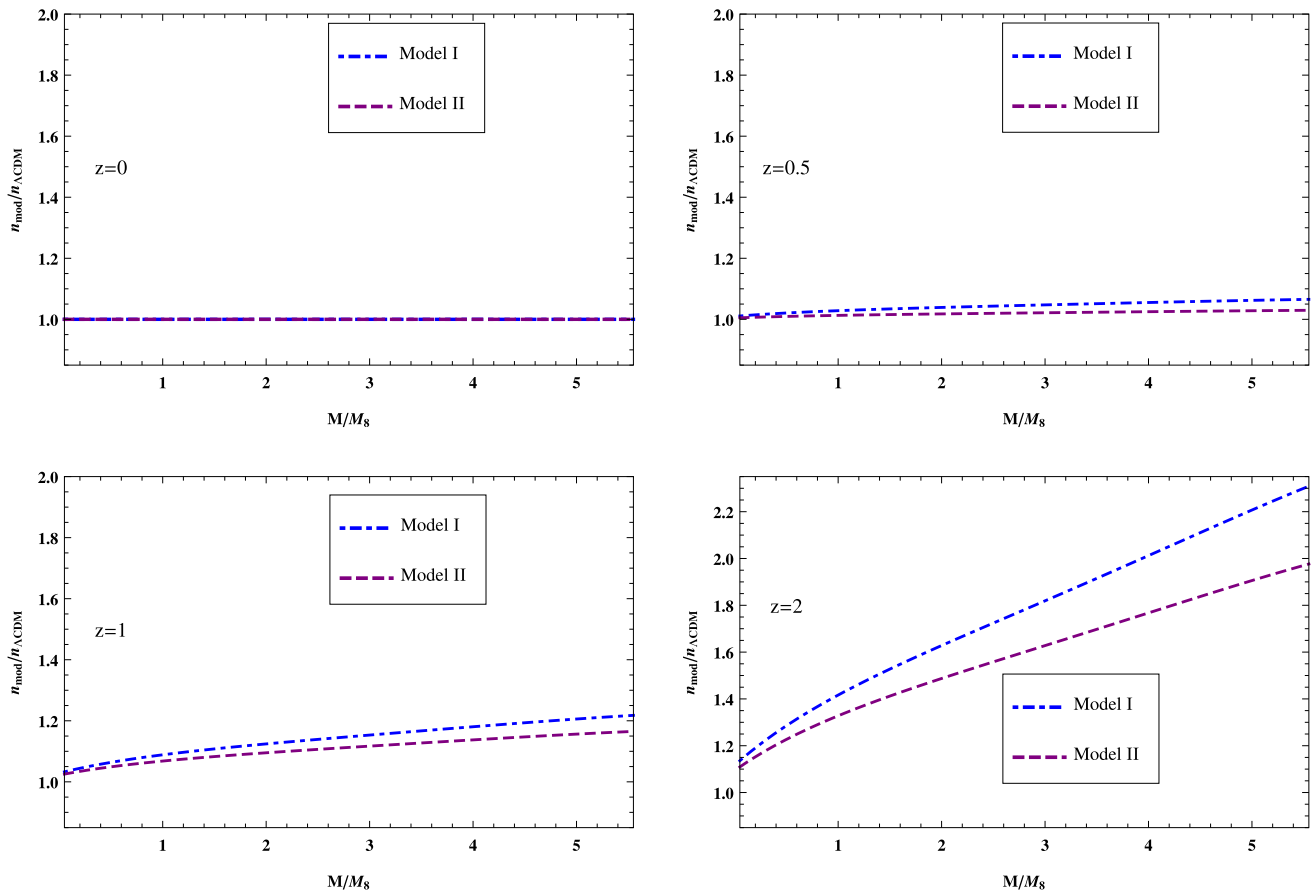


**Fig. 4** Ratio of the number of haloes above a given mass  $M$  between VG models (I, II) and concordance  $\Lambda$ CDM model evaluated at different redshifts:  $z=0$ ,  $z=0.5$ ,  $z=1$  and  $z=2$ , respectively, from up panel to bottom panel. Line style and colours are same as in Fig. 1

Fractional differences in the number of virialised haloes between different VG models and the concordance  $\Lambda$ CDM universe for three different mass scales:  $M > 10^{13} M_{\odot}/h$ ,  $M > 10^{14} M_{\odot}/h$ , and  $M > 10^{15} M_{\odot}/h$ , are reported in Table 2.

### 3.4 Some improvements on SCM in VG theory

Here we first extend the SCM in VG formalism by studying the effect of shear and rotation on the SCM parameters and then investigate how the number counts of massive clusters are changed by modification of mass function.

#### 3.4.1 The effect of shear and rotation

In standard SCM, we assume that haloes form due to the gravitational collapse of the initial spherical overdense region. This assumption is clearly a crude assumption. In fact, the initial perturbations are not completely spherical due to inclusion of shear and rotation (Bardeen et al. 1986; Del Popolo et al. 2001; Del Popolo 2002; Shaw et al. 2006; Bett et al. 2007). The general equations for the evolution of

perturbations in the presence of shear and rotation term have been presented in (Abramo et al. 2007; Pace et al. 2010). Also, the effect of shear and rotation on the evolution of overdensities in standard GR gravity has been studied for different DE models (Del Popolo et al. 2013a,b,c; Pace et al. 2014a). For the first time, the authors of (Del Popolo et al. 2013a) showed that including the shear and rotation term causes that the parameters of SCM are mass-dependent. Furthermore, the authors of (Del Popolo et al. 2013b) showed that the joint effect of shear and rotation is the slowing down of the collapse with respect to the simple SCM. Following (Del Popolo et al. 2013a,c; Pace et al. 2014a), we define the dimensionless quantity  $\alpha$  as the ratio between the rotational and the gravitational term as follows:

$$\alpha = \frac{L^2}{M^3 R G}, \tag{38}$$

where  $M$  and  $R$  are, respectively, the mass and the radius of the spherical overdense region and  $L$  is the angular momentum. The values of  $\alpha$  range from 0.05 for galactic mass scales ( $M \simeq 10^{11} M_{\odot} h^{-1}$ ) to  $3 \times 10^{-6}$  for cluster of galaxies scale ( $M \simeq 10^{15} M_{\odot} h^{-1}$ ). In the presence of shear and

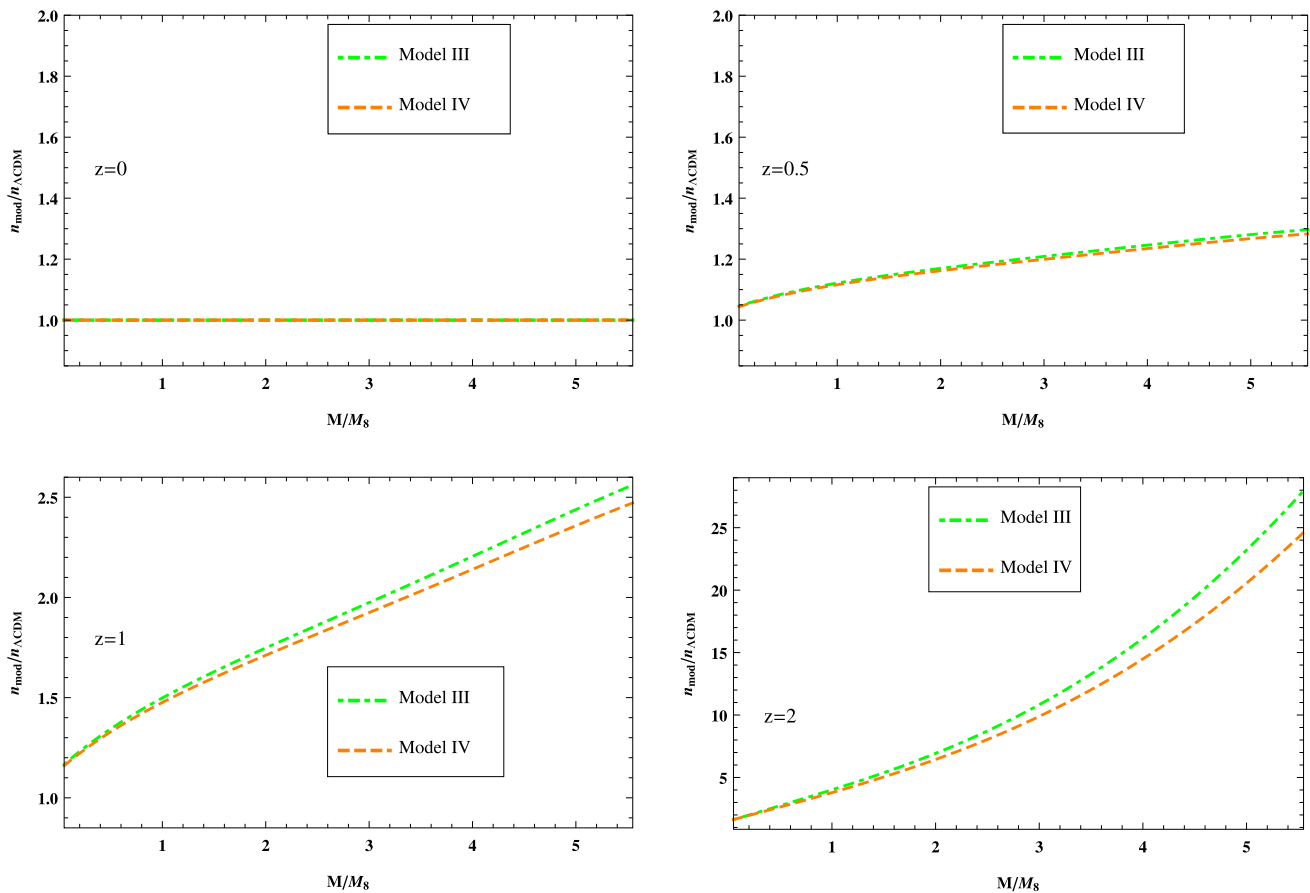


**Fig. 5** Ratio of the number of haloes above a given mass  $M$  between VG models (III, IV) and concordance  $\Lambda$ CDM model evaluated at different redshifts:  $z = 0, z = 0.5, z = 1$  and  $z = 2$ , respectively, from up panel to bottom panel. Line style and colours are same as in Fig. 1

rotation term, the equation for the evolution of non-linear overdensities (e.g., Eq. (27)) can be written as

$$\delta''_m + \left(\frac{3}{a} + \frac{E'}{E}\right)\delta'_m - \left(\frac{8 + 3\beta + \beta^2}{6 + 2\beta + \beta^2}\right)\frac{\delta'^2_m}{1 + \delta_m} - (1 - \alpha)(1 + \delta_m)\delta_m \times \left[\frac{(6 + 2\beta + \beta^2)(1 + \beta + \beta^2)}{(1 + \beta)(2 + \beta)^2} \frac{\Omega_{m0}}{E^2} a^{-\left(\frac{10+4\beta+\beta^2}{2+\beta}\right)}\right] = 0, \tag{39}$$

where the effect of  $\alpha$  on the evolution of non-linear overdensities appears on the last term in the left hand side of above equation. For complete discussion and derivations, see (Del Popolo et al. 2013b; Pace et al. 2014a). Note that the quantity  $\alpha$  is the non-linear parameter and therefore does not appear in linear Eq. (28). It has been shown that the effect of shear and rotation on the SCM at high redshifts is much smaller than present time (Pace et al. 2014a; Del Popolo et al. 2013b). Hence we focus on this effect on the SCM parameters only at the present time and calculate the present values of  $\delta_c$  and  $\Delta_{vir}$  by solving the non-linear Eq. (39). The results for different values of  $\alpha$  are collected in Table 3.

We see that both the linear overdensity  $\delta_c$  and virial overdensity  $\Delta_{vir}$  get higher values by increasing the shear and rotation parameter  $\alpha$ . We also see that the effect of shear and rotation on the collapsing sphere is more important at galactic scale ( $\alpha \simeq 0.05$ ) and is less important at massive cluster scales ( $\alpha \simeq 10^{-6}$ ). Both the above results are in agreement with those of the GR theory of gravity (e.g., see Pace et al. 2014a; Del Popolo et al. 2013b).

### 3.4.2 The effect of mass function

Here, we study that how changing the mass function affects the number counts of dark matter haloes. To do this, we calculate the number count of virialized haloes by adopting the new mass function presented by Del Popolo et al. (2017) which is in good agreement with simulations (Klypin et al. 2011; Bhattacharya et al. 2011). This new mass function is introduced as (Del Popolo et al. 2017):

$$vf(v) \simeq A_2 \sqrt{\frac{av}{2\pi}} \left(1 + \frac{0.1218}{(av)^{0.585}} + \frac{0.0079}{(av)^{0.4}} + \frac{0.1}{(av)^{0.45}}\right)$$

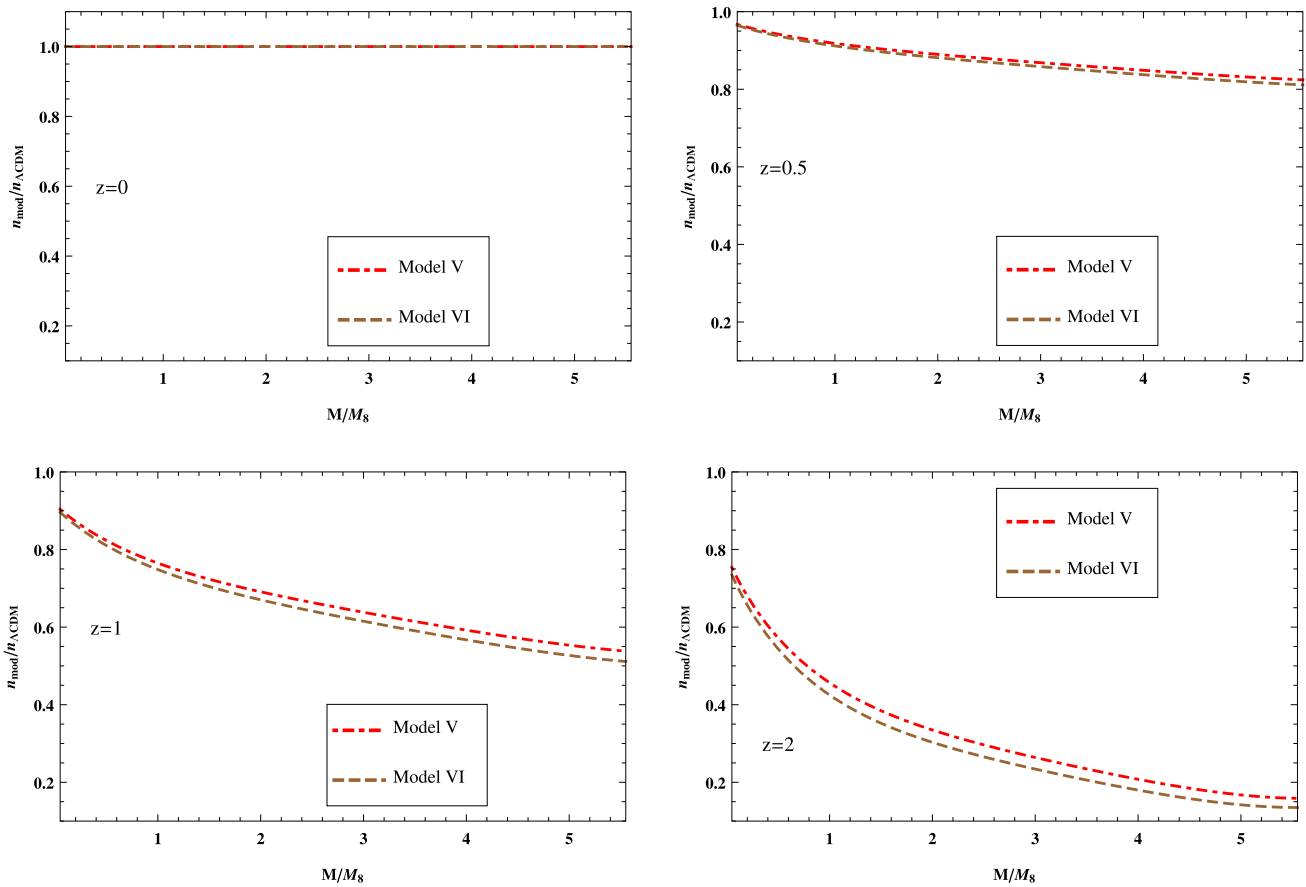


**Fig. 6** Ratio of the number of haloes above a given mass  $M$  between VG models (V, VI) and concordance  $\Lambda$ CDM model evaluated at different redshifts:  $z=0$ ,  $z=0.5$ ,  $z=1$  and  $z=2$ , respectively, from up panel to bottom panel. Line style and colours are same as in Fig. 1

$$\begin{aligned} & \times \exp \left[ -0.4019av^{2.12} \left( 1 + \frac{0.5526}{(av)^{0.585}} + \frac{0.02}{(av)^{0.4}} \right. \right. \\ & \left. \left. + \frac{0.07}{(av)^{0.45}} \right)^2 \right]. \end{aligned} \tag{40}$$

In this mass function, the effects of angular momentum and dynamical friction on the spherical collapse are included. Here, the numerical constants are  $A_2 = 0.93702$ ,  $a = 0.707$  and  $v = \delta_c/\sigma$ . In Fig. 7, we show the number of dark matter haloes in terms of  $M/M_8$  computed using the mass function by Del Popolo et al. (2017) normalized to its value computed by Sheth-Tormen mass function. In this figure,  $n_2$  and  $n_1$  are the number density of virialized haloes with mass above a given value  $M_1$  (see Eq. (37)) at collapse redshift  $z$  calculated using the mass function by Del Popolo et al. (2017) and Sheth-Tormen mass function, respectively. In general, we see that at low mass tail, the difference of the two mass functions is small. While at high mass tail, the difference is significant. We also see that the difference between the mass functions is increasing by redshift. The numerical results and the fractional differences of number of haloes above a given large mass  $M > 10^{15} M_\odot/h$  calcu-

lated for mass function by Del Popolo et al. (2017) and the Sheth-Tormen mass function are presented in Table 4.

## 4 Conclusion

In the context of VG theory, we firstly investigated the evolution of main cosmological quantities in background level and secondly studied the growth of cosmic structures using the spherical collapse model (SCM). We adopted the CPL parameterization and considered two different quintessence and phantom regimes for EoS parameter of DE. At background level, we found that, for all VG models considered in this work, the deceleration parameter  $q$  becomes negative at low redshifts. We also showed that in the context of VG theory, the transition from early decelerated to current accelerated expansion is consistent with observations.

In perturbation level, we calculated the growth of matter spherical overdensities in both linear and nonlinear regimes. In particular, we computed the evolution of linear overdensity parameter  $\delta_c$  and virial overdensity  $\Delta_{vir}$  as a function of cosmic redshift  $z$  for different VG models assumed in our

**Table 2** The fractional difference of number of haloes between cosmological models in VG cosmologies and the concordance  $\Lambda$ CDM model. Results are shown at four different redshifts:  $z = 0$ ,  $z = 0.5$ ,  $z = 1$  and  $z = 2$  for haloes with  $M > 10^{13}M_{\odot}/h$ ,  $M > 10^{14}M_{\odot}/h$ , and  $M > 10^{15}M_{\odot}/h$

Model I	$z = 0$	$z = 0.5$	$z = 1$	$z = 2$
$M > 10^{13}M_{\odot}/h$	0%	1%	2.8%	11.6%
$M > 10^{14}M_{\odot}/h$	0%	2.1%	6.5%	29.1%
$M > 10^{15}M_{\odot}/h$	0%	6.6%	21.87%	131.3%
Model II	$z = 0$	$z = 0.5$	$z = 1$	$z = 2$
$M > 10^{13}M_{\odot}/h$	0%	0.4%	2.2%	9.3%
$M > 10^{14}M_{\odot}/h$	0%	1%	5%	23.1%
$M > 10^{15}M_{\odot}/h$	0%	3%	16.6%	98%
Model III	$z = 0$	$z = 0.5$	$z = 1$	$z = 2$
$M > 10^{13}M_{\odot}/h$	0%	4%	14.3%	54.9%
$M > 10^{14}M_{\odot}/h$	0%	9%	35.1%	176.9%
$M > 10^{15}M_{\odot}/h$	0%	29.8%	156.6%	2702%
Model IV	$z = 0$	$z = 0.5$	$z = 1$	$z = 2$
$M > 10^{13}M_{\odot}/h$	0%	3.8%	13.7%	52.3%
$M > 10^{14}M_{\odot}/h$	0%	8.6%	33.6%	166.2%
$M > 10^{15}M_{\odot}/h$	0%	28.4%	147.7%	2364.4%
Model V	$z = 0$	$z = 0.5$	$z = 1$	$z = 2$
$M > 10^{13}M_{\odot}/h$	0%	-2.9%	-8.4%	-21.7%
$M > 10^{14}M_{\odot}/h$	0%	-6.2%	-18%	-43.5%
$M > 10^{15}M_{\odot}/h$	0%	-17.6%	-46.5%	-84.8%
Model VI	$z = 0$	$z = 0.5$	$z = 1$	$z = 2$
$M > 10^{13}M_{\odot}/h$	0%	-3.1%	-9.1%	-23.4%
$M > 10^{14}M_{\odot}/h$	0%	-6.7%	-19.3%	-46.4%
$M > 10^{15}M_{\odot}/h$	0%	-19%	-49.1%	-87.2%

analysis. Due to the effect of DE at low redshifts, we observed the decreasing of  $\delta_c$  and  $\Delta_{vir}$  along the cosmic redshift  $z$  in VG cosmologies similarly with that of the  $\Lambda$ CDM universe. Also, these quantities in VG theory tend to those of the EdS universe at enough high redshifts indicating that at early times the effects of DE are negligible.

In next step, we computed the abundance of virialized dark matter haloes in VG cosmologies using the Sheth-Tormen mass function. We saw that at lower redshifts the differences between the number of virialized haloes computed in VG theory and concordance  $\Lambda$ CDM universe are less (more) pronounced at low (high) mass tail of cosmic structures. While at higher redshifts, the difference is also considerable even at low mass tail of mass function. We

**Table 3** The numerical values for  $\delta_c$  ( $\Delta_{vir}$ ) calculated for different cosmological models in VG theory affected by including shear and rotation term

Model	$\alpha = 0.00$	$\alpha = 0.000001$	$\alpha = 0.001$	$\alpha = 0.05$
Model I	1.675 (103.17)	1.675 (103.17)	1.684 (103.24)	2.183 (107.17)
Model II	1.673 (100.09)	1.673 (100.09)	1.681 (100.17)	2.181 (103.98)
Model III	1.670 (117.20)	1.670 (117.20)	1.679 (117.29)	2.170 (121.74)
Model IV	1.667 (113.88)	1.668 (113.88)	1.676 (113.96)	2.169 (118.29)
Model V	1.680 (88.58)	1.680 (88.58)	1.688 (88.65)	2.194 (92.14)
Model VI	1.677 (85.79)	1.677 (85.79)	1.686 (85.86)	2.192 (89.25)
$\Lambda$ CDM	1.675 (101.90)	1.675 (101.90)	1.684 (101.97)	2.186 (105.74)

**Table 4** The fractional difference of number of haloes between the new mass function presented by Del Popolo et al. (2017) and the Sheth-Tormen mass function. Results are shown at four different redshifts:  $z = 0$ ,  $z = 0.5$ ,  $z = 1$  and  $z = 2$  for haloes with  $M > 10^{15}M_{\odot}/h$

$M > 10^{15}M_{\odot}/h$	$z = 0$	$z = 0.5$	$z = 1$	$z = 2$
Models I, II	13.19%	44.96%	123.19%	859.25%
Models III, IV	13.19%	42.31%	105.36%	583.56%
Models V, VI	13.19%	48.57%	145.24%	1301.38%

showed that in VG theory, like GR theory, the abundance of collapsed haloes in quintessence (phantom) DE models is higher (lower) than those of the  $\Lambda$ CDM cosmology. The impact of VG parameter  $\beta$  on the number density of virialized haloes is investigated. We observed that the VG models with negative sign of  $\beta$  have more collapsed objects rather than models with positive sign.

Finally, we extended the SCM in VG theory by investigating the effect of shear and rotation on the SCM parameters and studying the change of number count of dark matter haloes by modification of mass function. We found that  $\delta_c$  and  $\Delta_{vir}$  reach the larger values by increasing the shear and rotation parameter. Like standard gravity, in VG theory of gravity, the effect of shear and rotation on the galactic-size haloes is more pronounced than the massive cluster-size haloes. In addition, we found that the abundance of dark matter haloes at high mass tail computed by the new mass function Del Popolo et al. (2017) is higher than that of the Sheth-Tormen mass function while the difference is negligible at low mass tail.

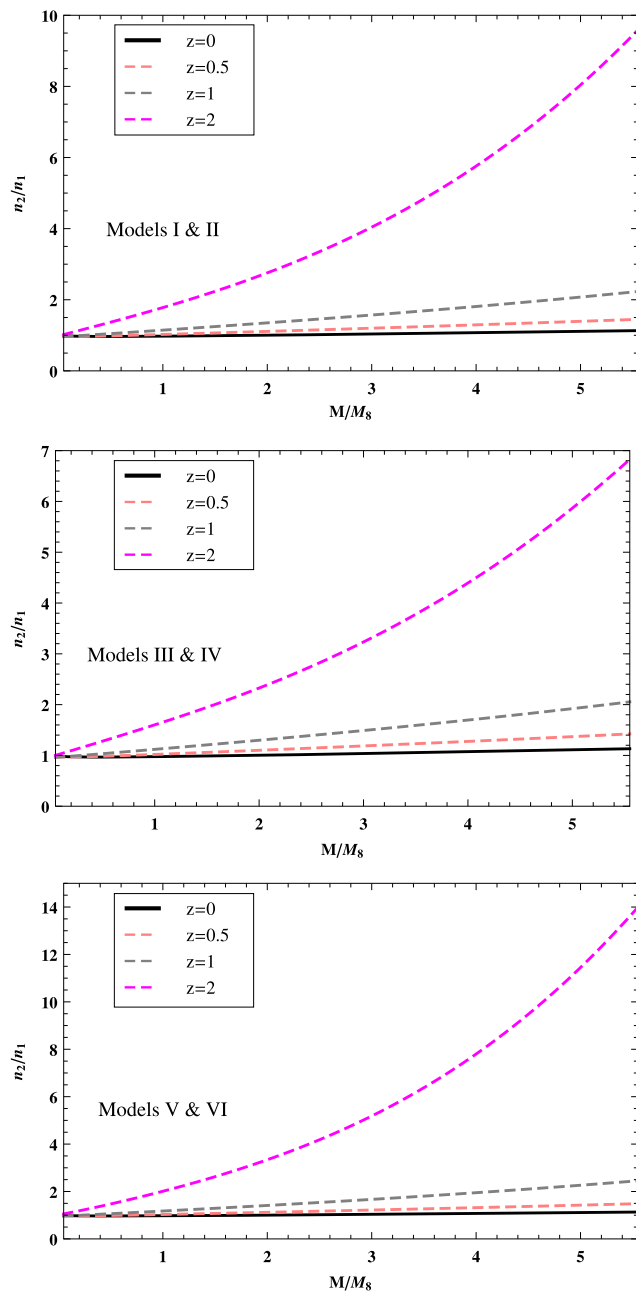


**Fig. 7** Ratio of the number of haloes above a given mass  $M$  between the new mass function presented in (Del Popolo et al. 2017) and Sheth-Tormen mass function at different cosmological redshifts  $z = 0.0$ ,  $z = 0.5$ ,  $z = 1.0$  and  $z = 2.0$  for VG models I & II (upper panel), VG models III & IV (middle panel) and VG models V & VI (lower panel)

**Publisher's Note** Springer Nature remains neutral with regard to jurisdictional claims in published maps and institutional affiliations.

## References

Abramo, L.R., Batista, R.C., Liberato, L., Rosenfeld, R.: *J. Cosmol. Astropart. Phys.* **11**, 12 (2007)

- Abramo, L.R., Batista, R.C., Liberato, L., Rosenfeld, R.: *Phys. Rev. D* **79**, 023516 (2009)
- Abramo, L.R., Batista, R.C., Rosenfeld, R.: *J. Cosmol. Astropart. Phys.* **7**, 40 (2009)
- Ade, P.A.R., et al.: *Astron. Astrophys.* **571**, 16 (2014)
- Ade, P.A.R., et al.: *Astron. Astrophys.* **594**, 14 (2016)
- Alavirad, H., Malekjani, M.: *Astrophys. Space Sci.* **349**, 967 (2014)
- Appleby, S.A., Linder, E.V., Weller, J.: *Phys. Rev. D* **88**, 043526 (2013)
- Arkani-Hamed, N., Creminelli, P., Mukohyama, S., Zaldarriaga, M.: *J. Cosmol. Astropart. Phys.* **04**, 001 (2004)
- Armendariz-Picon, C., Mukhanov, V.F., Steinhardt, P.J.: *Phys. Rev. D* **63**, 103510 (2001)
- Ascasibar, Y., Yepes, G., Gottlöber, S., Müller, V.: *Mon. Not. R. Astron. Soc.* **352**, 1109 (2004)
- Avila-Reese, V., Firmani, C., Hernández, X.: *Astrophys. J.* **505**, 37 (1988)
- Bardeen, J.M., Bond, J.R., Kaiser, N., Szalay, A.S.: *Astrophys. J.* **304**, 15 (1986)
- Barkana, R., Loeb, A.: *Phys. Rep.* **349**, 125 (2001)
- Basilakos, S., Voglis, N.: *Mon. Not. R. Astron. Soc.* **374**, 269 (2007)
- Basilakos, S., Sanchez, J.C.B., Perivolaropoulos, L.: *Phys. Rev. D* **80**, 043530 (2009)
- Basse, T., Bjaelde, O.E., Wong, Y.Y.Y.: *J. Cosmol. Astropart. Phys.* **1110**, 038 (2011)
- Batista, R.C., Pace, F.: *J. Cosmol. Astropart. Phys.* **1306**, 044 (2013)
- Benvenuto, O.G., Garcia-Berro, E., Isern, J.: *Phys. Rev. D* **69**, 082002 (2004)
- Bernardeau, F.: *Astrophys. J.* **433**, 1 (1994)
- Bertschinger, E.: *Astrophys. J. Suppl. Ser.* **58**, 39 (1985)
- Bett, P., Eke, V., Frenk, C.S., Jenkins, A., Helly, J., Navarro, J.: *Mon. Not. R. Astron. Soc.* **376**, 215 (2007)
- Bhattacharya, S., Heitmann, K., White, M., Lukic, Z., Wagner, C., Habib, S.: *Astrophys. J.* **732**, 122 (2011)
- Bond, J.R., Cole, S., Efstathiou, G., Kaiser, N.: *Astrophys. J.* **379**, 440 (1991)
- Brans, C.H., Dicke, R.H.: *Phys. Rev. D* **124**, 925 (1961)
- Bromm, V., Yoshida, N.: *Annu. Rev. Astron. Astrophys.* **49**, 373 (2011)
- Cai, R.G.: *Phys. Lett. B* **657**, 228 (2007)
- Caldwell, R.R.: *Phys. Lett. B* **545**, 23 (2002)
- Capozziello, S., Farooq, O., Luongo, O., Ratra, B.: *Phys. Rev. D* **90**(4), 044016 (2014)
- Capozziello, S., Luongo, O., Saridakis, E.N.: *Phys. Rev. D* **91**(12), 124037 (2015)
- Carroll, S.M.: *Living Rev. Relativ.* **380**, 1 (2001)
- Chevallier, M., Polarski, D.: *Int. J. Mod. Phys. D* **10**, 213 (2001)
- Ciardi, B., Ferrara, A.: *Space Sci. Rev.* **116**, 625 (2005)
- Copeland, E.J., Sami, M., Tsujikawa, S.: *Int. J. Mod. Phys. D* **15**, 1753 (2006)
- Copi, C.J., Davis, A.N., Krauss, L.M.: *Phys. Rev. Lett.* **92**, 171301 (2004)
- Damour, T., Gibbons, G.W., Taylor, J.H.: *Phys. Rev. Lett.* **61**, 1151 (1988)
- Del Popolo, A.: *Astron. Astrophys.* **387**, 759 (2002)
- Del Popolo, A., Ercan, E.N., Xia, Z.: *Astron. J.* **122**, 487 (2001)
- Del Popolo, A., Pace, F., Lima, J.A.S.: *Mon. Not. R. Astron. Soc.* **430**, 628 (2013a)
- Del Popolo, A., Pace, F., Maydanyuk, S.P., Lima, J.A.S., Jesus, J.F.: *Phys. Rev. D* **87**(4), 043527 (2013b)
- Del Popolo, A., Pace, F., Lima, J.A.S.: *Int. J. Mod. Phys. D* **22**, 1350038 (2013c)
- Del Popolo, A., Pace, F., Le Delliou, M.: *J. Cosmol. Astropart. Phys.* **1703**(03), 032 (2017)
- Devi, N.C., Sen, A.A.: *Mon. Not. R. Astron. Soc.* **413**, 2371 (2011)
- Eisenstein, D.J., Zehavi, I., Hogg, D.W., et al.: *Astrophys. J.* **633**, 560 (2005)

- Farooq, O., Madiyar, F.R., Crandall, S., Ratra, B.: *Astrophys. J.* **835**(1), 26 (2017)
- Fillmore, J.A., Goldreich, P.: *Astrophys. J.* **281**, 1 (1984)
- Freund, P.G.O.: *Nucl. Phys. B* **209**, 146 (1982)
- Gaztanaga, E., Garcia-Berro, E., Isern, J., Bravo, E., Dominguez, I.: *Phys. Rev. D* **65**, 023506 (2002)
- Guenther, D.B., Krauss, L.M., Demarque, P.: *Astrophys. J.* **498**, 871 (1998)
- Gunn, J.E., Gott, J.R.: *Astrophys. J.* **176**, 1 (1972)
- Guth, A.H.: *Phys. Rev. D* **23**, 347 (1981)
- Ho, S., Hirata, C., Padmanabhan, N., et al.: *Phys. Rev. D* **78**, 043519 (2008)
- Hoffman, Y., Shaham, J.: *Astrophys. J.* **297**, 16 (1985)
- Horellou, C., Berge, J.: *Mon. Not. R. Astron. Soc.* **360**, 1393 (2005)
- Jaffe, A.H., Ade, P.A., Balbi, A., Bock, J.J., et al.: *Phys. Rev. Lett.* **86**, 3475 (2001)
- Jarosik, N., Bennett, C.L., Dunkley, J., et al.: *Astrophys. J. Suppl. Ser.* **192**, 14 (2011)
- Jenkins, A., Frenk, C.S., White, S.D.M., Colberg, J.M., Cole, S., Evrard, A.E., Couchman, H.M.P., Yoshida, N.: *Mon. Not. R. Astron. Soc.* **321**, 372 (2001)
- Kaluza, T.: *Sitzungsber. Preuss. Akad. Wiss. Berlin (Math. Phys.)* **1921**, 966 (1921)
- Kamenshchik, A., Moschella, U., Pasquier, V.: *Phys. Lett. B* **511**, 265 (2001)
- Klypin, A., Trujillo-Gomez, S., Primack, J.: *Astrophys. J.* **740**, 102 (2011)
- Kolb, E.W., Perry, M.J., Walker, T.P.: *Phys. Rev. D* **33**, 869 (1986)
- Komatsu, E., Dunkley, J., Nolta, M.R., et al.: *Astrophys. J. Suppl. Ser.* **180**, 330 (2009)
- Komatsu, E., Smith, K.M., Dunkley, J., et al.: *Astrophys. J. Suppl. Ser.* **192**, 18 (2011)
- Kowalski, M., Rubin, D., Aldering, G., et al.: *Astrophys. J.* **686**, 749 (2008)
- Lahav, O., Lilje, P.B., Primack, J.R., Rees, M.J.: *Mon. Not. R. Astron. Soc.* **251**, 128 (1991)
- Li, M., Li, X.D., Wang, S., Zhang, X.: *J. Cosmol. Astropart. Phys.* **6**, 036 (2009)
- Lima, J.A.S., Marassi, L.: *Int. J. Mod. Phys. D* **13**, 1345 (2004)
- Linde, A.: *Phys. Lett. B* **238**, 160 (1990)
- Linder, E.V.: *Phys. Rev. Lett.* **90**, 091301 (2003)
- Linder, E.V.: *Phys. Rev. D* **72**, 043529 (2005)
- Loren-Aguilar, P., Garcia-Berro, E., Isern, J., Kubyshev, Yu.A.: *Class. Quantum Gravity* **20**, 3885 (2003)
- Lu, J., Xu, L., Tan, H., Gao, S.: *Phys. Rev. D* **89**, 063526 (2014)
- Maeda, K.-i.: *Class. Quantum Gravity* **3**, 233 (1986)
- Malekjani, M., Lu, J., Nazari-Pooya, N., Xu, L., Mohammad-Zadeh Jassur, D., Honari-Jafarpour, M.: *Astrophys. Space Sci.* **360**, 24 (2015a)
- Malekjani, M., Naderi, T., Pace, F.: *Mon. Not. R. Astron. Soc.* **453**, 4148 (2015b)
- Malekjani, M., Haidari, N., Basilakos, S.: *Mon. Not. R. Astron. Soc.* **466**(3), 3488 (2017)
- Maor, I., Lahav, O.: *J. Cosmol. Astropart. Phys.* **7**, 3 (2005)
- Mehrabi, A., Pace, F., Malekjani, M., Del Popolo, A.: *Mon. Not. R. Astron. Soc.* **465**(3), 2687 (2017)
- Mota, D.F., van de Bruck, C.: *Astron. Astrophys.* **421**, 71 (2004)
- Naderi, T., Malekjani, M., Pace, F.: *Mon. Not. R. Astron. Soc.* **447**, 1873 (2015)
- Nazari-Pooya, N., Malekjani, M., Pace, F., Jassur, D.M.-Z.: *Mon. Not. R. Astron. Soc.* **458**, 3795 (2016)
- Nesseris, S., Perivolaropoulos, L.: *Phys. Rev. D* **77**, 023504 (2008)
- Nojiri, S., Odintsov, S.D.: *Phys. Lett. B* **562**, 147 (2003)
- Ohta, Y., Kayo, I., Taruya, A.: *Astrophys. J.* **589**, 1 (2003)
- Ohta, Y., Kayo, I., Taruya, A.: *Astrophys. J.* **608**, 647 (2004)
- Pace, F., Waizmann, J.C., Bartelmann, M.: *Mon. Not. R. Astron. Soc.* **406**, 1865 (2010)
- Pace, F., Fedeli, C., Moscardini, L., Bartelmann, M.: *Mon. Not. R. Astron. Soc.* **422**, 1186 (2012)
- Pace, F., Batista, R.C., Del Popolo, A.: *Mon. Not. R. Astron. Soc.* **445**, 648 (2014a)
- Pace, F., Moscardini, L., Crittenden, R., Bartelmann, M., Pettorino, V.: *Mon. Not. R. Astron. Soc.* **437**, 547 (2014b)
- Padmanabhan, T.: *Cosmology and Astrophysics Through Problems*. Cambridge University Press, Cambridge, England (1996)
- Padmanabhan, T.: *Phys. Rep.* **380**, 235 (2003)
- Peebles, P.J.E.: *Principles of Physical Cosmology*. Princeton University Press, Princeton, USA (1993)
- Peebles, P.J., Ratra, B.: *Rev. Mod. Phys.* **75**, 559 (2003)
- Percival, W.J., et al.: *Mon. Not. R. Astron. Soc.* **353**, 1201 (2004)
- Percival, W.J., Reid, B.A., Eisenstein, D.J., et al.: *Mon. Not. R. Astron. Soc.* **401**, 2148 (2010)
- Perlmutter, S., et al.: *Astrophys. J.* **517**, 565 (1999)
- Piazza, F., Tsujikawa, S.: *J. Cosmol. Astropart. Phys.* **07**, 004 (2004)
- Press, W.H., Schechter, P.: *Astrophys. J.* **187**, 425 (1974)
- Reed, D., Bower, R., Frenk, C., Jenkins, A., Theuns, T.: *Mon. Not. R. Astron. Soc.* **374**, 2 (2007)
- Rezaei, M., Malekjani, M.: *Phys. Rev. D* **96**, 063519 (2017)
- Riess, A.G., Filippenko, A.V., et al.: *Astron. J.* **116**, 1009 (1998)
- Riess, A.G., et al.: *Astrophys. J.* **607**, 665 (2004)
- Ryden, B.S., Gunn, J.E.: *Astrophys. J.* **318**, 15 (1987)
- Sahni, V., Starobinsky, A.: *Int. J. Mod. Phys. D* **9**, 373 (2000)
- Seljak, U., et al.: *Phys. Rev. D* **71**, 103515 (2005)
- Sen, A.: *J. High Energy Phys.* **04**, 048 (2002)
- Shaw, L., Weller, J., Ostriker, J.P., Bode, P.: *Astrophys. J.* **646**, 815 (2006)
- Sheth, R.K., Tormen, G.: *Mon. Not. R. Astron. Soc.* **308**, 119 (1999)
- Sheth, R.K., Tormen, G.: *Mon. Not. R. Astron. Soc.* **329**, 61 (2002)
- Starobinsky, A.A.: *Phys. Lett. B* **91**, 99 (1980)
- Subramanian, K., Cen, R., Ostriker, J.P.: *Astrophys. J.* **538**, 528 (2000)
- Tegmark, M., et al.: *Phys. Rev. D* **69**, 103501 (2004)
- Thomas, S.: *Phys. Rev. Lett.* **89**, 081301 (2002)
- Turyshev, S.G., Williams, J.G., Nordvedt, K. Jr., Shao, M., Murphy, T.W. Jr.: *Lect. Notes Phys.* **648**, 311 (2004)
- Viana, P.T.P., Liddle, A.R.: *Mon. Not. R. Astron. Soc.* **281**, 323 (1996)
- Wang, L., Steinhardt, P.J.: *Astrophys. J.* **508**, 483 (1998)
- Wang, Y., Tegmark, M.: *Phys. Rev. D* **71**, 103513 (2005)
- Weinberg, S.: *Rev. Mod. Phys.* **61**, 1 (1989)
- Williams, L.L.R., Babul, A., Dalcanton, J.J.: *Astrophys. J.* **604**, 18 (2004)
- Wintergerst, N., Pettorino, V.: *Phys. Rev. D* **82**, 103516 (2010)